HIGHLIGHTS OF THE STRUCTURE OF OUR GALAXY

(NRAO Summer Student Lecture Notes - 1978)

by

P. F. Bowers

I. INTRODUCTION

A cursory glance at the late summer sky can quickly provide us with insight into the structure of our Galaxy. The broad band of diffuse light known as the Milky Way roughly defines the plane of the Galaxy and can easily be resolved into a myriad of stars. At higher galactic latitudes the number of stars per square degree rapidly decreases, reaching a minimum near the galactic poles. Early discussions of galactic structure were not much more sophisticated than this, and early workers quickly concluded that we live in a pancake-shaped system of many stars with the Sun in the plane. Moreover, measurements of the number density of stars in the galactic plane indicated that this density rapidly decreases in all directions at large distances from the Sun. The conclusion was that the Sun was not only in the plane but at the center of the Galaxy. This pre-Copernican notion was in the mainstream of scientific thinking as late as 1930!

Of course this interpretation was not without its difficulties, among them being the distribution of globular clusters which showed a strong concentration about 35000 light years from the Sun in the direction of Sagittarius. The globular clusters were also strangely missing from regions within a few degrees of the galactic plane, though at higher latitudes they were symmetrically distributed above and below the plane. Perhaps even more disconcerting was the apparent "increase" in the linear diameters of open clusters at distances farther from the Sun.

These problems were resolved as soon as the reddening effects of interstellar dust were properly appreciated. The high degree of reddening ($\gtrsim 1$ mag. kpc^{-1} in visual light) and the strong concentration of dust to the galactic plane are essential factors to be considered in optical studies of galactic structure and unfortunately, severely limit most optical studies to within only a few kpc of the Sun. Fortunately, however, studies of other galactic systems, the advent of radio astronomy, and more recently, technological developments in other spectral windows lead to a picture of the large-scale structure of the Galaxy which complements the more restricted regions available to optical observers.

II. SPIRAL STRUCTURE

A. Neutral Hydrogen

There are many lines of evidence which suggest our Galaxy is probably a spiral system, but our location in the plane of the Galaxy makes it difficult to study the spiral structure. It is apparent from studies of other galaxies that spiral arms are delineated by regions of young stars, HII regions, dust lanes, and concentrations of interstellar gas. The spiral arms represent global regions of active star formation, and thus to investigate the spiral structure we must concern ourselves with these "young" ($< 10^8$ yr) spiral tracers.

Fig. 1 summarizes an optical picture of spiral structure where various spiral tracers have been plotted in a polar diagram centered at the Sun. There is considerable scatter in the diagram, but there appear to be at least three apparent features labelled as the Sagittarius, Orion, and Perseus arms respectively. The limitations of optical studies of spiral structure are made clear in this diagram which only concerns itself with structure within a few kpc of the Sun.

In contrast, radio observations of various galactic species provide useful information about the large-scale structure and thus complement the optical studies. In particular, spectral line studies of the gas (HI, HII, CO, and numerous other molecules) provide a means to determine the radial velocity and ultimately an approximate distance to the gas.

Fig. 2 shows the geometry of the situation. The observed radial velocity V can be related to the distance R by

$$V = R_o \left(\frac{\Theta(R)}{R} - \frac{\Theta_o}{R_o}\right) \sin \ell$$

where R_o is the Sun-center distance (10 kpc), $\Theta(R)$ is the rotational velocity at distance R, Θ_o is the velocity in the solar neighborhood (250 km s^{-1}), and ℓ is the galactic longitude. The above relation assumes a differentially rotating system where the orbits are circular. To use this relation to get distances we must first obtain the rotation curve $\Theta(R)$, which, in turn, is related to the overall mass distribution of the Galaxy. From Fig. 2 the maximum radial velocity occurs when the line of sight is tangent to the orbit at $R = R_{min} = R_o \sin \ell$. For this case

$$V_{max} = \Theta(R_o \sin \ell) - \Theta_o \sin \ell,$$

so that V_{max} directly yields $\Theta(R_o \sin \ell)$ for a given ℓ.

Fig. 3 summarizes the results of such analyses 21-cm HI in the northern and southern hemispheres for the region 4-10 kpc from the galactic center. There are two important aspects of these curves which should be noted: a) the northern and southern curves are displaced, and b) the curves are wavy. Neither of these results should be expected for curves giving the "circular" velocity as a function of R for an axisymmetric galaxy. These effects are likely due to noncircular velocity components of the gas due to streaming motions. There is ample evidence that such motions exist and that they are accentuated in the presence of spiral arms. Such noncircular motions make derived kinematic distances to features less certain and thus make it more difficult to map the spiral structure. Ironically, it is the evidence of streaming motions which indicates large-scale gravitational perturbations and which may be the best evidence that our Galaxy has spiral structure.

Another serious problem for mapping spiral structure is velocity crowding effects whereby the intensity of a feature at a given velocity is due to low density gas at many different distances rather than a concentration of gas (e.g., a spiral arm) at a well-defined distance. There are many regions of the Galaxy where the velocity gradient due to rotation is small (e.g., $\ell = 0°$) and this effect dominates the observations. The importance of such effects has been demonstrated by an extreme (non-physical) example where it has been shown that a galaxy with a uniformly constant density but with velocity streaming and crowding effects could produce the observational data as well as a galaxy in which there are density enhancements due to spiral structure.

Fig. 4 shows the observed HI intensities as a function of galactic longitude and radial velocity. The utility of such diagrams is that only observed quantities are plotted and thus the diagrams are model independent. The effects of galactic rotation are clearly apparent in this diagram. The figure also shows evidence for large-scale features which span many degrees of longitude, even though these features can be quite clumpy.

By converting the velocities of these features to kinematic distances, maps of spiral structure such as that in Fig. 5 are derived. Of particular interest are the prominent Norma-Scutum and Sagittarius spiral arms at $R \simeq 5$ and 8 kpc respectively. There are also numerous other features, but many of these are not well defined in the $\ell - v$ diagram and thus are uncertain in the polar plot. For example, Fig. 6 shows an alternative picture also derived from the HI data by determining kinematic distances. Several of the more prominent features are still present, but their pitch angles differ from those of the previous figures. There is also substantial disagreement about the placement or existence of many smaller features, particularly outside the solar circle. This diagram is also interesting because it compares the optical and HI pictures of spiral structure and demonstrates rather poor agreement between the two.

Because of the difficulties inherent to the kinematic distance technique, a newer approach to mapping spiral structure is the model-fitting approach whereby a theoretical model of spiral structure is fit to the data by accounting for the gravitational perturbations (and velocity effects) introduced by the spiral arms. Fig. 7 shows such a model of spiral structure. The overall pattern is basically two-armed inside the solar circle and shows major features which are also present in the previous diagrams. The outer regions show two features (the Carina and Outer arms) which are out of phase with the basic pattern and may suggest a multiple-armed structure. Multiple arms might be caused, for example, by secondary shock, between the major arms.

To put these models in perspective, Fig. 8 shows the HI distribution for the relatively well defined spiral galaxy M51. It is clear that HI is associated with the optical arms, but it is certainly not confined to them. In particular, the large concentrations of HI at distances well beyond the spiral features should be noted. The HI complexes are patchy and irregular, and it is not difficult to imagine the problems an astronomer situated in the disk of this galaxy would have in mapping the spiral structure via neutral hydrogen. It is also easy to see how local irregularities could cause conflicting interpretations between optical and radio views of this structure. In addition to these problems most spirals are not nearly so well defined, but may have irregular arms, multiple arms, bar structures, etc.

The proposed spiral features for our Galaxy do not extend to the galactic center, but stop at about $R \simeq 4$ kpc. Fig. 9 shows an $\ell - v$ diagram of the inner region of the Galaxy and depicts several notable features, however.

The 4-kpc expanding arm feature extends from $\ell \sim 340°$, $v \sim -100$ km s^{-1} to $\ell \sim 6°$, $v \sim 0$ km s^{-1}, crossing $\ell = 0°$ at the noncircular velocity of -53 km s^{-1}. HI profiles toward the galactic center show this feature in absorption, indicating it is between the Sun and the galactic center. Recent CO surveys also indicate the presence of the feature to $\ell \sim 23°$.

Near $\ell = 0°$, there are also relatively strong emission features at positive velocities up to ~200 km s^{-1}. This gas does not appear in absorption against Sgr A and thus lies behind it. The feature has been denoted as the +135 km s^{-1} expanding arm and extends from about $-6°$ to $+12°$.

Yet another prominent feature in this region is the rapidly rotating nuclear disk at $|\ell| < 4°$ with very high negative velocities at $\ell < 0°$ and positive velocities at $\ell > 0°$. Because of the sudden cutoff of the feature at $\ell = 0°$, it is assumed to be a rotating feature rather than an expanding feature.

The nature and extent of these features are not well understood. Fig. 10 shows a sketch of the possible situation. The noncircular velocities of some of these features have stimulated much speculation that they are expanding due to an explosive origin at the galactic center. An alternative explanation is that these features may be gas trapped in resonance regions of the Galaxy. Indeed the spiral density-wave theory suggests such a region (the inner Lindblad resonance) at $R \simeq 4$ kpc. These features may also be related to a bar structure, as indicated in the sketch, but the evidence for, and understanding of such a bar is very poor.

B. Species Other Than HI

So far we have been concerned with the large-scale distribution of HI as a tracer of spiral structure. Though the data available for HI is much more complete than for other galactic species, recent work has provided many interesting points of comparison between these species and HI.

One particularly advantageous probe is CO which, like HI, is sufficiently intense and ubiquitous to be detected over large regions of the Galaxy. Also, CO observations complement those of HI since the CO is located in the dense, colder regions of the interstellar medium and provides an indirect measure of the distribution of molecular hydrogen.

An interesting comparison of the CO and HI distributions over the same region of sky is shown in Figs. 11a and 11b. Both species show many of the same features (the rotating nuclear disk, the 4-kpc arm, etc.) but there are also significant differences. The CO is much more clumpy than the HI and there is a notable lack of CO emission at negative velocities for $\ell > 0°$. This indicates that the CO is, for the most part, confined to regions inside the solar circle, since large negative velocities at these longitudes imply distances $R > 10$ kpc; observations at $\ell > 90°$ also confirm the concentration of CO to the inner Galaxy. Detailed comparisons of the CO and HI data also indicate that HI self-absorption features are often associated with CO emission features, confirming the association of CO with cold material.

Fig. 12 compares the radial distributions of CO and HI at $b = 0°$. As suggested by the $\ell - v$ diagrams, the CO is confined to the inner regions ($R \lesssim 10$ kpc) while the HI is more widely distributed. The CO shows a strong and relatively narrow abundance peak at about R = 5 kpc while the HI is distributed almost as a plateau from about 5 to 13 kpc. There is a low abundance of both species at $R \lesssim 4$ kpc.

Fig. 13 compares the radial mass distributions of HI, H_2 (inferred from CO) and the total mass distribution (σ_t) as derived from a mass model of the Galaxy. In addition to the obvious differences in the distributions, it is of interest to note the ratio of gas (HI + H_2) to total mass is roughly constant (~4%) through a large part of the Galaxy. The high percentages of CO and H_2 in the inner Galaxy suggest that processes which lead to the formation of these molecules (and eventually to possible star formation) are more efficient in this region of the Galaxy.

This view is supported by the radial distributions of several other galactic species which are young or associated with young objects. For example, Fig. 14 shows the distributions of ionized hydrogen, gamma-radiation (related to supernovae and cosmic rays), and supernova remnants. All these species have radial distributions similar to CO. Thus the HI distribution, once considered to be the prototype distribution for the young components of the Galaxy, now appears to be a singular distribution.

Despite the apparent singularity of the HI distribution, the above discussion is not an argument against spiral structure, but does necessitate a reasonable self-consistent explanation for the different distributions. It is thus useful to consider the density-wave theory of spiral structure.

C. The Density-Wave Theory

The density-wave theory is a particularly attractive model for spiral structure because it is a global theory and can be used to explain the regularity and symmetry of large-scale structures (the grand design), despite the fact that on smaller scales these arms consist of clumps and patches of material which can make them appear quite irregular. It also provides a means of "permanence" for the spiral structure. If the spiral arms always consisted of the same stars, they would quickly wind up due to differential galactic rotation. The density-wave theory is also attractive because it makes definite predictions about the distribution and kinematics of material associated with spiral arms, and in several cases these predictions have been verified.

The basic idea is that at any moment of time, the spiral arms represent the local maxima of a wave of density which is caused and supported by gravitational effects. The density wave rigidly rotates with some pattern speed Ω_p while the stars and gas are differentially rotating with angular velocities $\Omega\,(R)$. As the gas hits the density wave, it is subject to some degree of compression which depends on the value of $(\Omega\,(R) - \Omega_p)$ - i.e., the larger this value, the larger the compression. Massive clouds of molecules and dust (and ultimately stars) can be formed. The dust is preferentially located at the inner edges of the arms (assuming $\Omega > \Omega_p$) while the newly formed high-luminosity stars and associated HII regions delineate the arms. The material continues to move through the density wave and the luminous spiral tracers evolve rapidly (~ 10^7 yr or 1/10 of a rotation period) to later type objects. Thus the spiral features represent a "snapshot" in time of the locus of luminous objects recently formed due to the compression initiated by the density wave. Because the density wave is a local minimum in the gravitational potential, it also causes systematic deviations of the mean velocities of gas and stars from pure circular rotation and so we get velocity streaming.

For the density wave to be more than a transient phenomenon, a self-consistent solution must be provided, whereby the stars maintain the field at the same time they respond to it. Fig. 15 illustrates the results of such calculations, where A and B are spiral arms, the shaded circle represents an unperturbed stellar orbit, the solid ellipse represents the perturbed orbit in a rotating reference frame, and the dashed ellipses represent two adjacent stellar orbits. The numbers 1-4 represent points of intersection for the perturbed and unperturbed orbits. Between points 1 and 2, the star(or gas cloud) feels arm A more strongly than B and is pulled outward while its velocity decreases relatively to the circular velocity. Eventually the star is pulled back in, speeding past position 2 to position 3 where the cycle begins again. The star's velocity is lowest at the apogalactica but this is not the density maximum because adjacent orbits are too far apart at these points. The maximum occurs at positions 2 and 4 because adjacent orbits lie closest together at these points. Because of this and because the stars lie along spiral arms for ~ 3/4 of their orbits, their velocity pattern reinforces the density wave.

From comparison of the density-wave calculations to observations of HI, a likely pattern speed for our Galaxy is ~13.5 km s^{-1} kpc^{-1}. For most of the Galaxy $\Omega > \Omega_p$, so stars and gas move through the density wave. The gas feels the perturbations (~ 5% of the average field) much more strongly than the stars, and noncircular velocity components of ~ 10 km s^{-1} can be produced for the gas (compared to ~ 1 km s^{-1} for the stars).

Since the Galaxy is differentially rotating while the density wave is rigidly rotating, the velocity at which the gas moves through the density wave varies with distance from the galactic center. Fig. 16 shows the result of this in terms of the velocity component $W_{\perp o}$ perpendicular to the density wave. Since the degree of compression depends on $W_{\perp o}$, the figure is equivalently showing the compression as a function of R. For example, $W_{\perp o} = 0$ when $\Omega = \Omega_p$ at the corotation point R_c. For smaller R, Ω increases while Ω_p is constant. Thus $W_{\perp o}$ (and the compression) becomes larger. Relatively strong compression is expected in the inner Galaxy where $W_{\perp o} > a$, the sound speed of the interstellar medium. Moreover, the accumulated effect of the compression is larger because the frequency at which the gas hits the wave pattern increases. Thus gas in the inner regions is subject to stronger, more frequent compressions which can initiate star formation. For R $\lesssim$ 4 kpc, however, little, if any, star formation is expected because of the inner Lindblad resonance - the point at which first-order calculations of the density wave are no longer valid. In addition, there is very little gas available for star formation in this region.

In many ways it is easier to test the density-wave theory for other galaxies than for our own since our view of the Galaxy is edge-on and is not an optimum position from which to derive a grand design of spiral structure. Applications of the density-wave theory to nearly face-on spirals have been very successful in describing the morphological characteristics of spiral structure (e.g., dust lanes on the inner edges of the arms due to compression of the gas and dust clouds) as well as the associated streaming motions (less than the circular velocity on the inner edges of arms and in excess of the circular velocity on the outer edges). In addition the HI distribution for many other spiral galaxies (such as M51) extends well beyond the visible signs of spiral structure, while the HII regions are essentially confined to the inner parts of the galaxies. All this does not imply that the density-wave theory is not without its problems (e.g., how does the density wave originate?), but it is certainly the most viable theory of spiral structure presently at hand.

III. THE BULK OF THE GALAXY

Thus far we have been primarily concerned with the component of the Galaxy associated with spiral structure (i.e., gas and luminous stars, but to keep a proper perspective we must remember that while this component may be very prominent, it represents $\lesssim$ 10% of the mass. The bulk of the Galaxy consists of low-luminosity, relatively old stars, as can be inferred from Table 1 where mass densities in the solar neighborhood are given for various objects.

The components of the Galaxy are commonly discussed in terms of population types -- a concept originated by Baade from observations of M31 during the 1940's. Extreme Population I objects (molecular clouds, HII regions, OB stars, etc.) are closely associated with spiral structure and regions of star formation, while Extreme Population II objects (such as globular clusters) are among the oldest objects in the Galaxy and are distributed throughout the halo. Intermediate populations are distributed in the disk. About 70% of the mass is in the disk component while ~20% is attributed to the halo component.

Table 2 summarizes some examples and properties of these population types. The conclusion is that the distributions and motions of various species are reasonably well correlated with their age. Those objects with higher orbital eccentricities, larger Z velocities (perpendicular to the plane), larger scale heights, stronger concentrations to the galactic center, and low metal abundances tend to be among the oldest objects in the Galaxy. Of course, there are always exceptions -- e.g., high-velocity stars which are metal rich -- but the overall picture is consistent with a relatively rapid collapse of the protogalaxy ($\sim 2 \times 10^{11}\ M_\odot$) about 15×10^9 yr ago. Net rotation of the protogalaxy provided an angular momentum axis. Cloud-cloud collisions dampened their relative motions and resulted in the formation of a flattened gaseous disk perpendicular to the axis. Collision rates for stars forming during the collapse were negligible, however, so the oldest stars (and globular clusters) distributed in the halo retained their original orbits.

Star formation and metal enrichment via supernovae subsequently proceeded in the disk component. Perturbations of the orbits of disk stars presumably by massive interstellar clouds resulted in an increase of their velocity dispersion and scale height with time. Determination of the present values for these parameters thus provides information about the ages of the various galactic components.

A SHORT BIBLIOGRAPHY

Blaauw, A., and Schmidt, M. (ed.): Galactic Structure, U. Chicago Press, (1965).

Mihalis, D.: Galactic Astronomy, W. H. Freeman and Co., (1968).

Chiu, H., and Muriel, A. (ed.): Galactic Astronomy, Vols. 1 and 2., Gordon and Breach, (1970).

Mavridis, L. N. (ed.): Structure and Evolution of the Galaxy, D. Reidel Publ. Co., (1971).

Kerr, F. J., and Simonson, S. C. (ed.): Galactic Radio Astronomy, D. Reidel Publ. Co., (1974).

Wielen, R.: "Density-Wave Theory of Spiral Structure of Galaxies", Publications of the Astronomical Society of the Pacific, **86**, 341, (1974).

Freeman, K. C.: "Stellar Dynamics and the Structure of the Galaxy", in Galaxies and the Universe, U. Chicago Press, (1975).

Burton, W. B.: "The Morphology of Hydrogen and Other Tracers in the Galaxy", Annual Review of Astronomy and Astrophysics, **14**, 275, (1976).

Oort, J. H.: "The Galactic Center", Annual Review of Astronomy and Astrophysics, **15**, 295, (1977).

Optical spiral structure of our Galaxy. The Sun is at the center of the diagram. The galactic center is in the direction toward 0° galactic longitude at a distance of 10 kiloparsecs from the Sun. The principal observed sections of the Sagittarius, Orion, and Perseus Arms are shown. The directions from the Sun toward some of the key constellations along the band of the Milky Way are marked along the periphery of the diagram. (A diagram based on data from W. Becker and Th. Schmidt-Kaler.)

Fig. 1

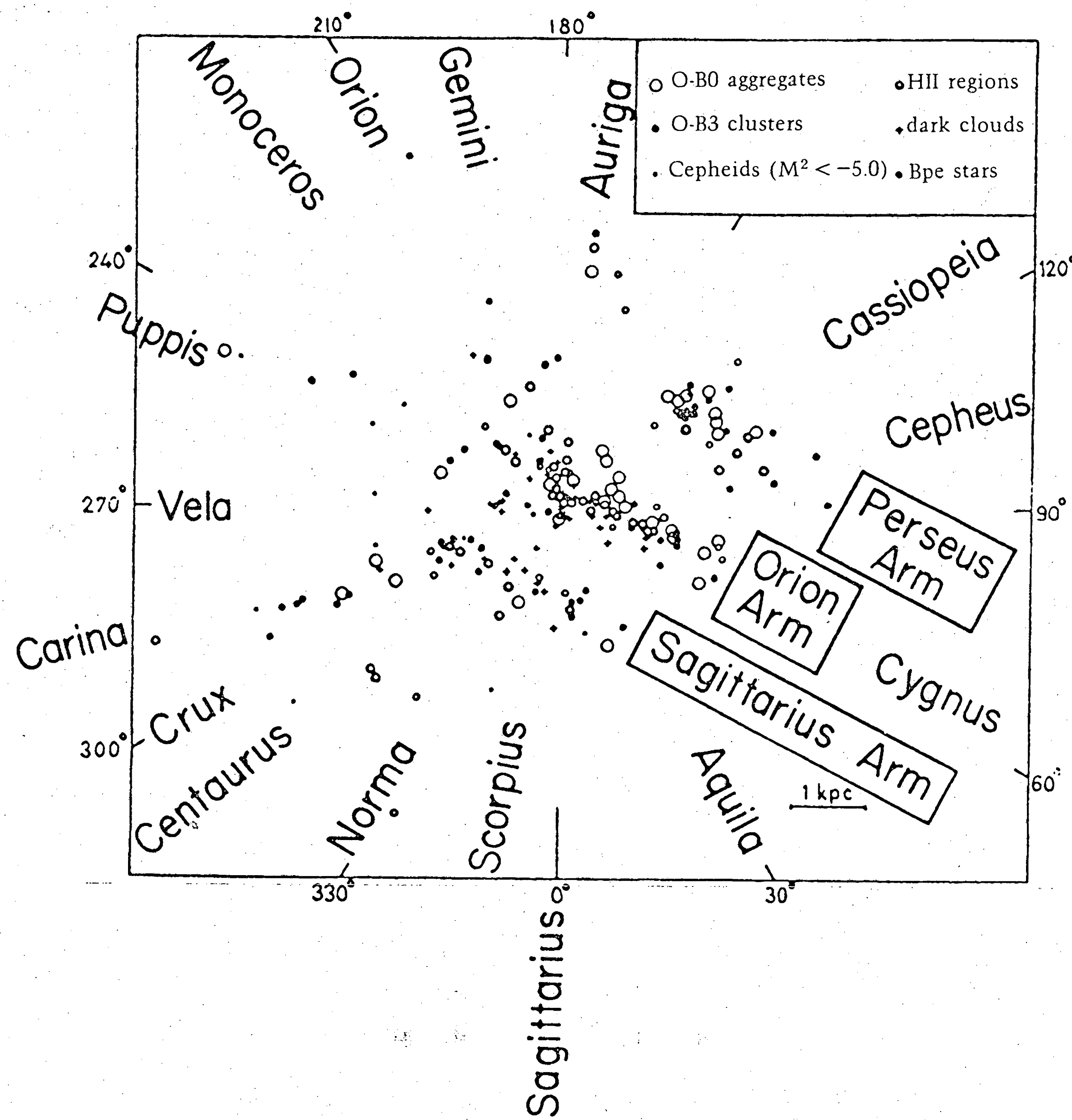

Galactic Rotation/The Oort Geometry. Here the Sun, the galactic center, and a star define the galactic plane; all orbital motions are circular. The various symbols are defined in the text.

FIG. 2

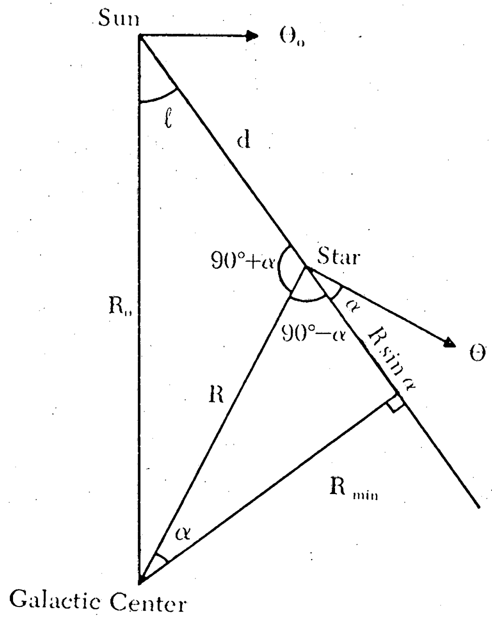

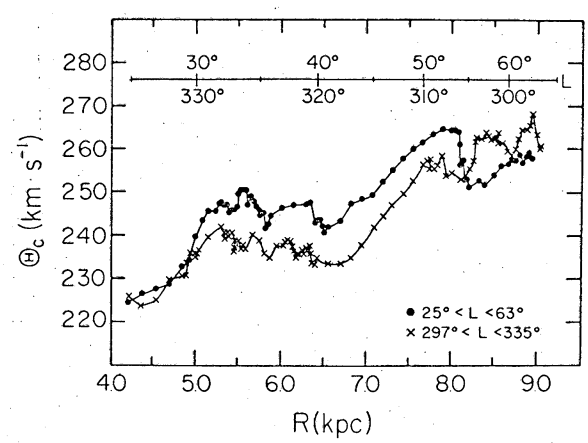

Kerr's two rotation curves. The galactic rotation curves for northern and southern sides of the galactic center have been derived from tangential 21-centimeter radio observations assuming circular rotation. The lack of smoothness of each curve and the differences between the curves are now being interpreted as caused by large-scale streaming associated with spiral features.

FIG. 3

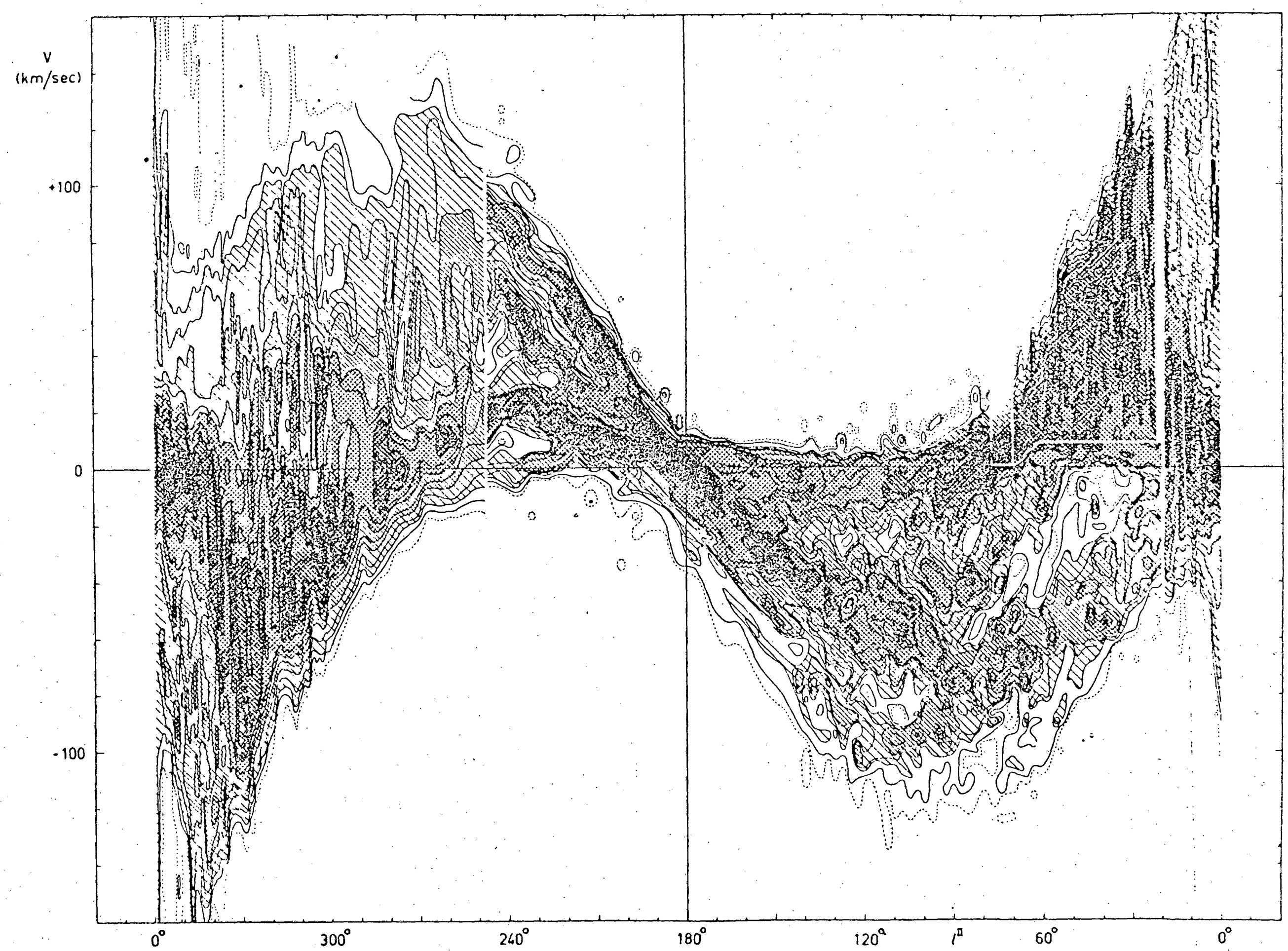

21-cm line of our Galaxy.

FIG. 4

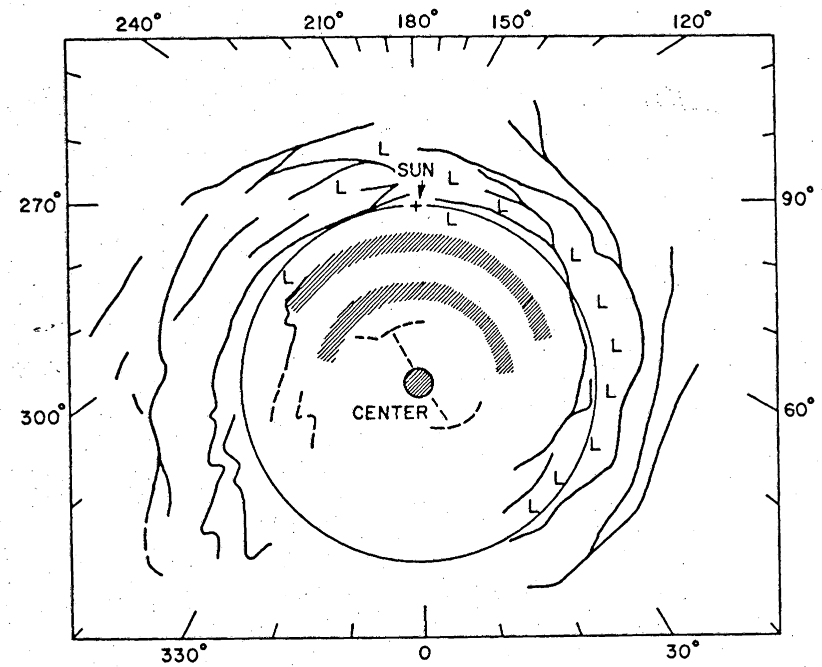

SKETCH OF GALACTIC HYDROGEN SPIRAL STRUCTURE

The Spiral Structure of Our Galaxy from 21-cm Data. This is a sketch of the neutral hydrogen distribution in the galactic plane, as deduced by Kerr, Hindman, and Henderson. The spiral structure is clearly visible (though complex). The paucity of structure near $\ell = 0°$ and $\ell = 180°$ is due to the large uncertainties in distances in these directions. The symbol L indicates regions of *low* hydrogen density.

FIG. 5

A preliminary map of radio spiral structure. Harold F. Weaver made this radio map on the basis of the Hat Creek 21-centimeter survey. It represents only the preliminary analysis (1972) of an extensive body of basic data. For comparison, Weaver has entered the optical data (see Fig. 103) of Becker and Schmidt-Kaler. The probable extensions of the observed features to the southern Milky Way (unobservable from Hat Creek Observatory, in California) have been sketched by Weaver.

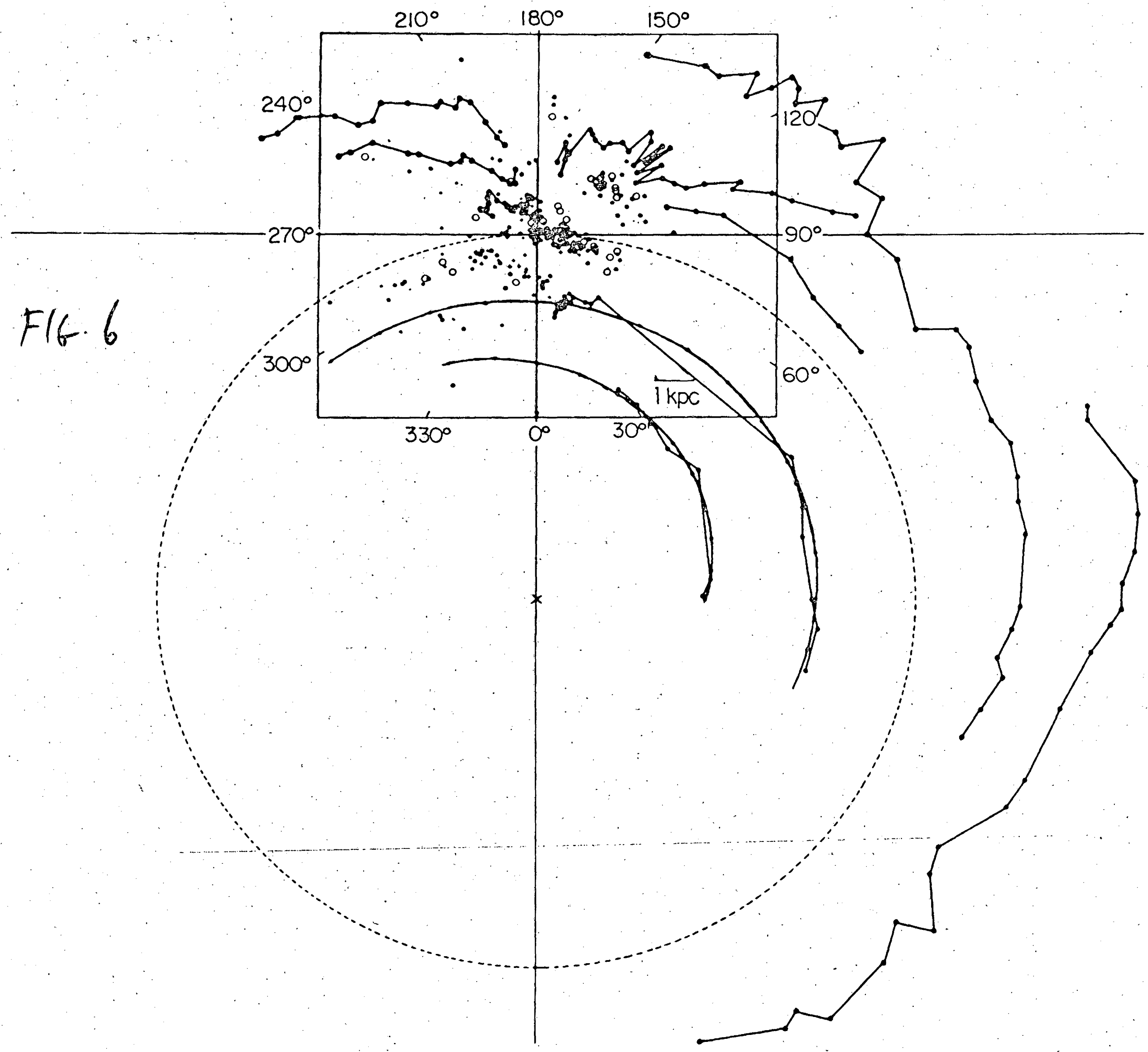

FIG. 6

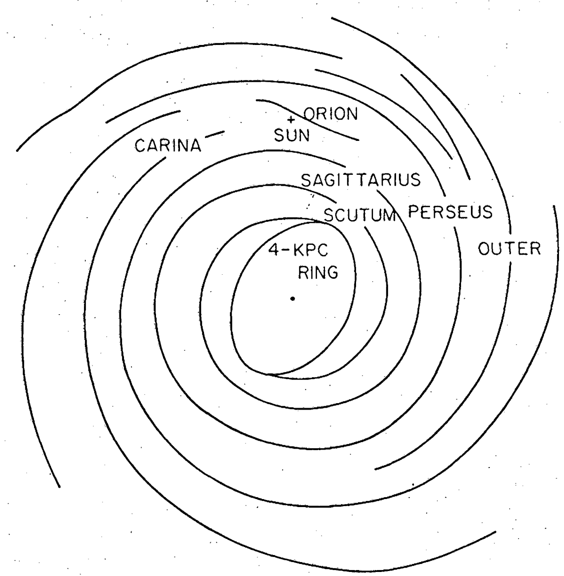

Final version of spiral map, with the addition of the 4-kpc dispersion ring from Simonson and Mader (1973)

FIG. 7

Equal-intensity contours for 21-centimeter radiation produced by neutral atomic hydrogen in the spiral galaxy Messier 51. The contours are shown superposed on a print of the 200-inch Hale reflector photograph reproduced in Fig. 115. Preliminary results with the Westerbork Array shown to B. J. Bok by Dr. Ernst Raimond (November 13, 1972).

FIG. 8

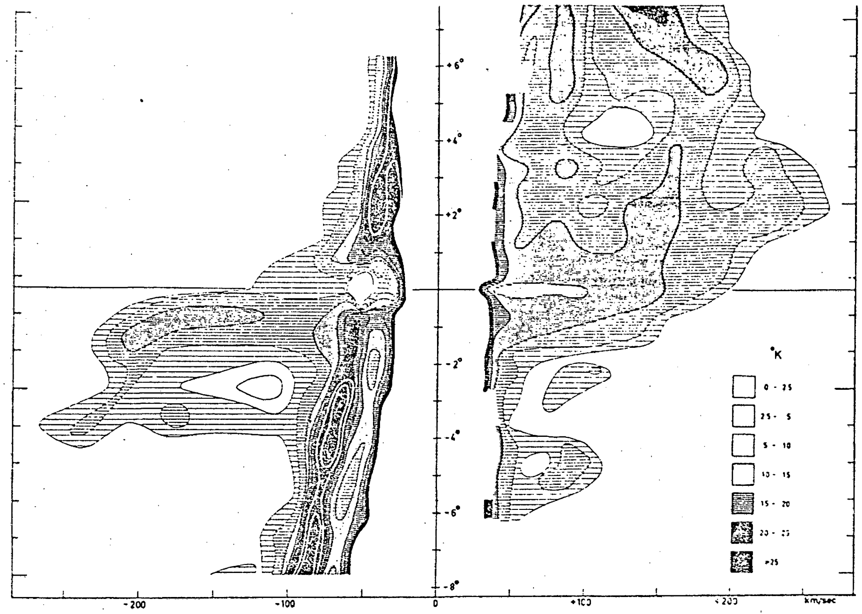

Velocity-longitude contours of atomic hydrogen in the galactic plane between $-8°$ and $+8°$ longitude, observed with the Dwingeloo radiotelescope with a half-power beam of 34′ (Rougoor 1964).

FIG. 9

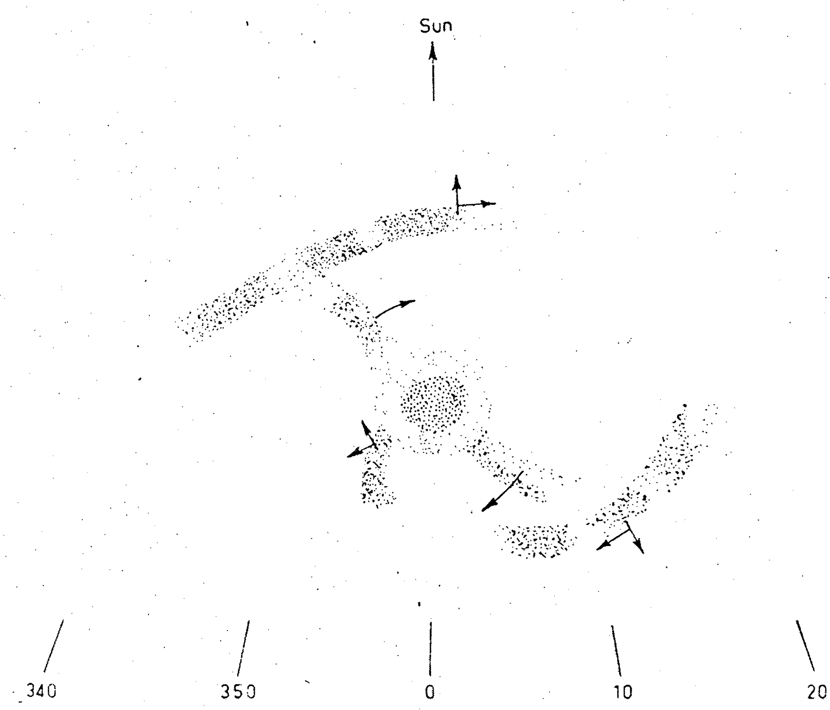

Neutral Hydrogen Near the Galactic Center. A model of the galactic-center region, showing the expanding 3-kpc spiral arm, the high-velocity barred structure, and the central gas disk.

FIG. 10

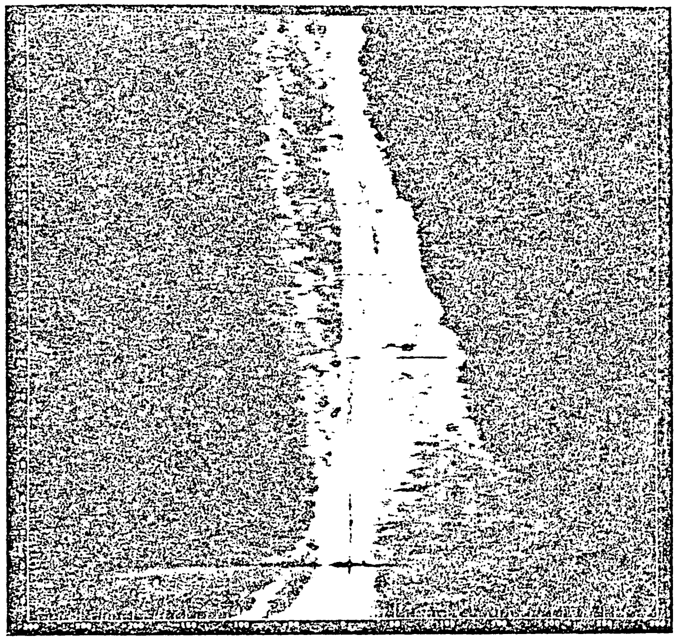

Grey-scale representation of HI emission intensities in longitude-velocity coordinates at the galactic equator. Westerhout (1976) made the observations at $\ell \geq 2°$; Bania (1977) made those at $\ell < 2°$. For comparison with the CO situation, the scale is the same as in Figure 1. The HI observations similarly sample every 0°2 and their velocity resolution is 1.3 km s^{-1}. The HI galactic disk has a diameter approximately twice that of the CO disk. In the region where the CO and HI distributions overlap, the two tracers show the same kinematics. The CO distribution is evidently clumpier than that of the HI.

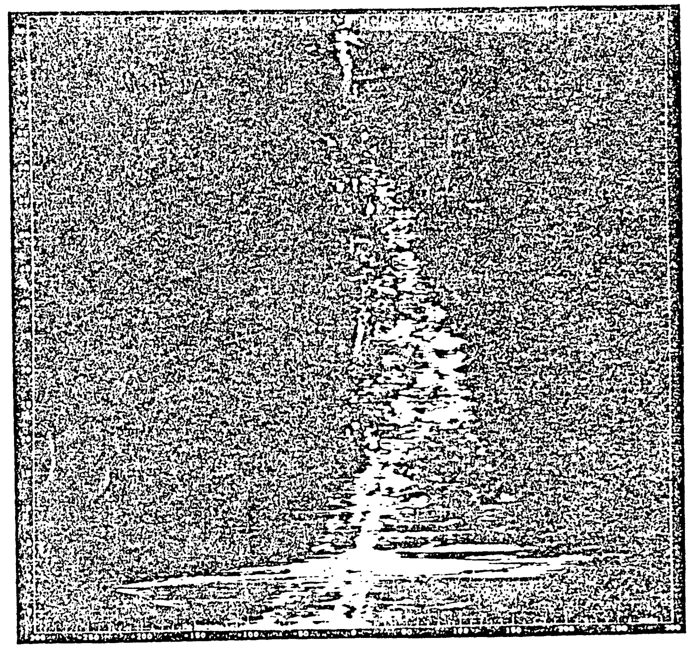

Grey-scale representation of $^{12}C^{16}O$ emission intensities in longitude-velocity coordinates at the galactic equator. Little CO emission occurs in the portions of this figure corresponding to R > 9 kpc (except for the exceptional Cygnus region) or to R < 4 kpc (except for the exceptional 3-kpc arm and the intense nuclear sources). The observations at $\ell < 10°$ are due to Bania (1977), those at $10° < \ell < 36°$ to Gordon and Burton (1976), and those at $\ell > 36°$ to Burton and Gordon (1977). The sampling interval of 0°2 sets the angular resolution; the velocity resolution is 1.3 km s^{-1} at $\ell \geq 10°$ and 2.6 km s^{-1} at $\ell < 10°$.

FIG. 11

FIG. 12

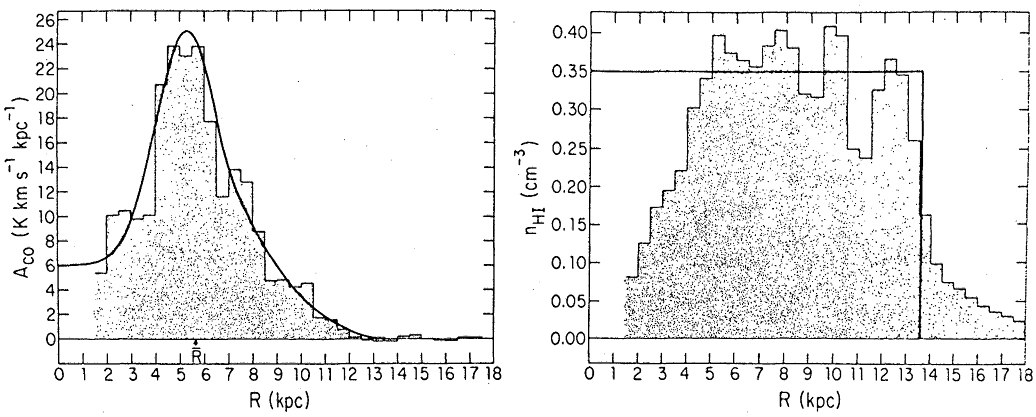

(left) Radial distribution of CO emission at b = 0° expressed as the accumulated total emission in galactic annuli. The galactic-plane distributions of most Population I constituents follow the form of the CO distribution. The line is a smoothed approximation to the measured histogram. (right) Radial distribution of HI column densities at b = 0°

FIG. 13

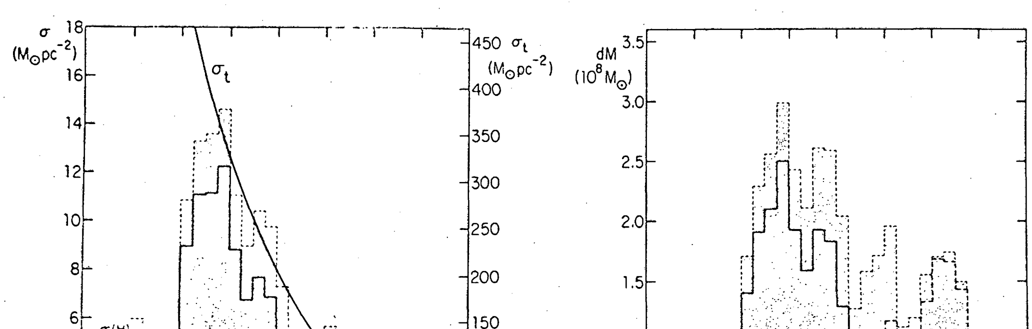

Radial distribution of projected surface densities (left) and of differential masses (right) of atomic and molecular hydrogen (Gordon and Burton 1976). At smaller distances hydrogen in molecular form dominates the mass distribution of the interstellar gas; at larger distances most of the interstellar gas is in the form of atomic hydrogen. Also shown is the total surface density σ_t predicted by Innanen

FIG. 14

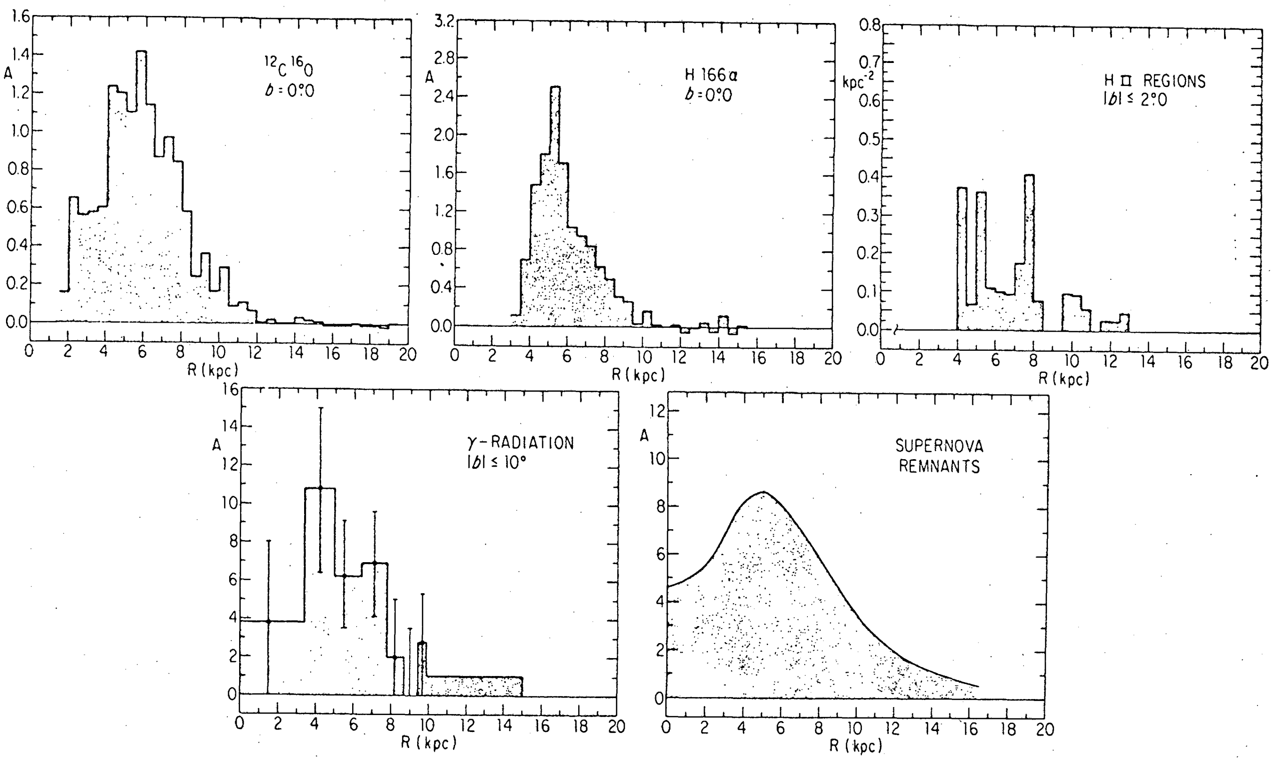

Radial distributions of several constituents of the galactic disk.

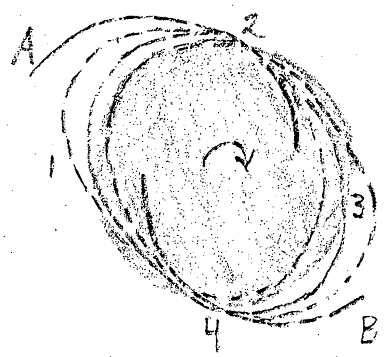

FIG. 15

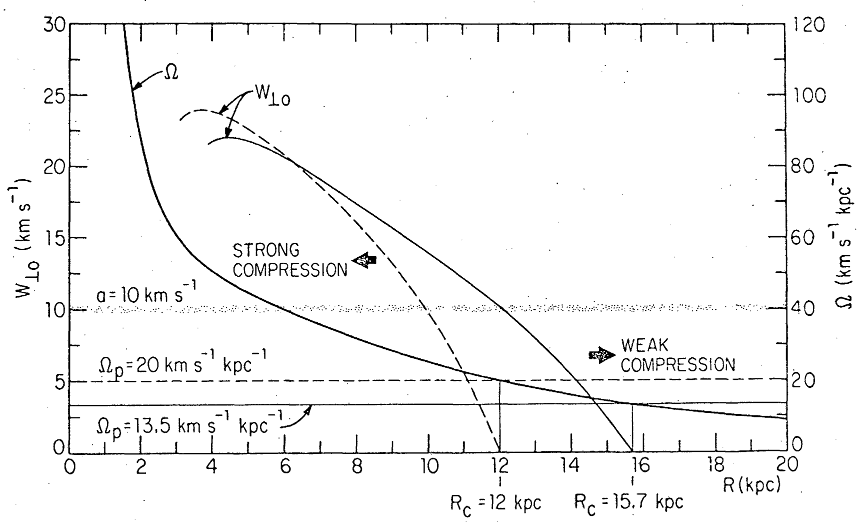

Schematic representation of some of the characteristics of a density-wave model of our Galaxy (after W. W. Roberts et al. 1975). The quantity $\Omega(R) = \Theta(R)/R$ is the basic angular velocity of differential rotation; two plausible values of the constant angular velocity of the wave pattern, Ω_p, are indicated. The velocity components, $W_{\perp o}$, of basic rotation normal to a spiral arm are shown for the two values of Ω_p. Relatively strong compression is expected in the inner Galaxy where $W_{\perp o} > a$, the effective acoustic speed in the interstellar medium. The frequency at which the galactic shock wave acts on the gas, $2[\Omega(R) - \Omega_p]$, also enhances the compression effects in the inner Galaxy.

FIG. 16

Table 1

Mass Densities of Various Objects

Object	Mass density ($10^{-3}\mathfrak{M}_\odot$ per pc^3)	Object	Mass density ($10^{-3}\mathfrak{M}_\odot$ per pc^3)
O–B	0.9	White dwarfs	8
A	1	Subdwarfs	1.5
F	3	Long-period variables	0.001
dG	4	RR Lyrae	10^{-5}
dK	9	Cepheids	0.001
dM	29	Planetary nebulae	5×10^{-6}
gG	0.8	Galactic clusters	0.04
gK	0.1	Globular clusters	0.001
gM	0.01		

Table 2

Characteristics of Stellar Populations

	Population Group				
	EXTREME POPULATION I	OLDER POPULATION I	DISK POPULATION II	INTERMEDIATE POPULATION II	HALO POPULATION II
Typical Objects	Interstellar dust and gas O and B stars Supergiants T Tauri stars Young open clusters Classical Cepheids O-associations H II regions	Sun Strong-line stars A stars Me dwarfs Giants Older open clusters	Weak-line stars Planetary nebulae Galactic bulge Novae RR Lyrae stars ($P < 0.4$ day)	High-velocity stars ($Z > 30$ km sec^{-1}) Long-period variables ($P < 250$ days)	Globular clusters Extreme metal-poor stars (subdwarfs) RR Lyrae stars ($P > 0.4$ day) Population II Cepheids
Characteristics					
$\langle\|z\|\rangle$, pc	120	160	400	700	2000
$\langle\|Z\|\rangle$, km sec^{-1}	8	10	17	25	75
Distribution	Extremely patchy in spiral arms	Patchy	Smooth	Smooth	Smooth
Age (10^9 yr)	<0.1	0.1 to 10	3 to 10	~ 10	$\gtrsim 10$
Brightest stars (M_{vis})	-8	-5	-3	-3	-3
Concentration to galactic center	None	Little	Considerable	Strong	Strong
Galactic orbits	Circular	Almost circular	Slightly eccentric	Eccentric	Highly eccentric